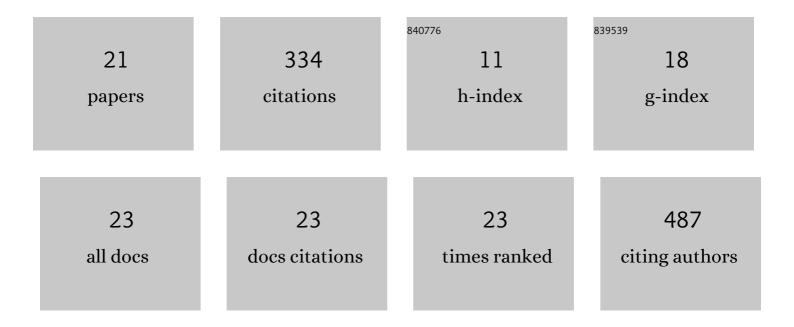
Wybe J M Van Der Kemp

List of Publications by Year in descending order

Source: https://exaly.com/author-pdf/7718626/publications.pdf Version: 2024-02-01



#	Article	IF	CITATIONS
1	Feasibility of 31 P spectroscopic imaging at 7 T in lung carcinoma patients. NMR in Biomedicine, 2021, 34, e4204.	2.8	10
2	Comparison of 2-Hydroxyglutarate Detection With sLASER and MEGA-sLASER at 7T. Frontiers in Neurology, 2021, 12, 718423.	2.4	9
3	Inherently decoupled ^{1} H antennas and ^{31} P loops for metabolic imaging of liver metastasis at 7 T . NMR in Biomedicine, 2020, 33, e4221.	2.8	7
4	SNR optimized ³¹ P functional MRS to detect mitochondrial and extracellular pH change during visual stimulation. NMR in Biomedicine, 2019, 32, e4137.	2.8	10
5	Analysis of chemical exchange saturation transfer contributions from brain metabolites to the Z-spectra at various field strengths and pH. Scientific Reports, 2019, 9, 1089.	3.3	40
6	Contradiction between amide EST signal and pH in breast cancer explained with metabolic MRI. NMR in Biomedicine, 2019, 32, e4110.	2.8	20
7	Early detection of changes in phospholipid metabolism during neoadjuvant chemotherapy in breast cancer patients using phosphorus magnetic resonance spectroscopy at 7T. NMR in Biomedicine, 2019, 32, e4086.	2.8	20
8	Shortening of apparent transverse relaxation time of inorganic phosphate as a breast cancer biomarker. NMR in Biomedicine, 2019, 32, e4011.	2.8	8
9	³¹ PT ₂ s of phosphomonoesters, phosphodiesters, and inorganic phosphate in the human brain at 7T. Magnetic Resonance in Medicine, 2018, 80, 29-35.	3.0	14
10	Proton and phosphorus magnetic resonance spectroscopy of the healthy human breast at 7ÂT. NMR in Biomedicine, 2017, 30, e3684.	2.8	14
11	Glycerophosphocholine and Glycerophosphoethanolamine Are Not the Main Sources of the In Vivo31P MRS Phosphodiester Signals from Healthy Fibroglandular Breast Tissue at 7 T. Frontiers in Oncology, 2016, 6, 29.	2.8	13
12	Proton observed phosphorus editing (POPE) for <i>in vivo</i> detection of phospholipid metabolites. NMR in Biomedicine, 2016, 29, 1222-1230.	2.8	10
13	Saturation-transfer effects and longitudinal relaxation times of ³¹ P metabolites in fibroglandular breast tissue at 7T. Magnetic Resonance in Medicine, 2016, 76, 402-407.	3.0	3
14	2D AMESING multi-echo 31P-MRSI of the liver at 7T allows transverse relaxation assessment and T2-weighted averaging for improved SNR. Magnetic Resonance Imaging, 2016, 34, 219-226.	1.8	4
15	Dynamic contrast-enhanced breast MRI at 7T and 3T: an intra-individual comparison study. SpringerPlus, 2016, 5, 13.	1.2	9
16	Multiparametric MRI With Dynamic Contrast Enhancement, Diffusion-Weighted Imaging, and 31-Phosphorus Spectroscopy at 7 T for Characterization of Breast Cancer. Investigative Radiology, 2015, 50, 766-771.	6.2	31
17	Radiofrequency configuration to facilitate bilateral breast31P MR spectroscopic imaging and high-resolution MRI at 7 Tesla. Magnetic Resonance in Medicine, 2015, 74, 1803-1810.	3.0	26
18	MRI and ³¹ P magnetic resonance spectroscopy hardware for axillary lymph node investigation at 7T. Magnetic Resonance in Medicine, 2015, 73, 2038-2046.	3.0	10

#	Article	IF	CITATIONS
19	1H/31P Polarization Transfer at 9.4 Tesla for Improved Specificity of Detecting Phosphomonoesters and Phosphodiesters in Breast Tumor Models. PLoS ONE, 2014, 9, e102256.	2.5	14
20	Detection of alterations in membrane metabolism during neoadjuvant chemotherapy in patients with breast cancer using phosphorus magnetic resonance spectroscopy at 7 Tesla. SpringerPlus, 2014, 3, 634.	1.2	17
21	Quantitative ³¹ P magnetic resonance spectroscopy of the human breast at 7 T. Magnetic Resonance in Medicine, 2012, 68, 339-348.	3.0	45